

PESSTO SDDR4 : ESO Phase 3 Data Release Description

Data Collection	PESSTO
Release Number	6
Data Provider	Stephen J. Smartt
Date	24.02.2021

Abstract

PESSTO (Public ESO Spectroscopic Survey of Transient Objects) ran from April 2012 - April 2017 on the New Technology Telescope using the instruments EFOSC2 and SOFI. An extension of PESSTO project (ePESSTO) then ran from April 2017 - April 2019. We typically targeted supernovae and optical transients brighter than 20.5^m for classification and selected science targets for detailed follow-up. We used standard EFOSC2 setups providing spectra with resolutions of 13-17Å between 3680-10320Å. A subset of the brighter science targets was selected for SOFI spectroscopy with the blue and red grisms (resolutions 23-33Å) and imaging with broadband JHK_s filters. In the following, we define SDDR4 as the set of data products from April 2012 to April 2019, covering the seven years of PESSTO/ePESSTO operations. This release includes the EFOSC2 and SOFI spectra, reduced SOFI images and the PESSTO Transient Catalogue (a catalogue of all PESSTO sources with a meaningful¹ spectral classification) all obtained during the seven years of PESSTO/ePESSTO operations.

Overview of Observations

PESSTO/ePESSTO² was allocated 90-100 nights per year, in visitor mode, on the ESO NTT. There were no observations planned during the months the Galactic centre is at optimal right ascension which make it difficult to search for extragalactic SNe and there is also large time pressure from the ESO community for Milky Way stellar science. PESSTO was typically allocated 10 nights per month split into three sub-runs of 4N, 3N and 3N. Typically the middle sub-run is dark time, while the two others are grey/bright with the moon up for around 50% of the time. The instruments are EFOSC2 and SOFI and both spectroscopy and imaging modes are employed. The PESSTO collaboration host public webpages with useful information in the form of night reports, observing conditions, observing with the NTT, and the data reduction pipeline. This information is updated during the survey and users should read this document with the information on www.pessto.org and the wiki pages that the homepage points to. A summary of the spectroscopic data setups is given in Tables 1 and 2. The science target selection strategy is described in detail in Smartt et al. (2015).

¹ Very occasionally PESSTO obtains spectra for which no object trace is found, or the signal-to-noise is so poor as to be essentially meaningless

² From here forward the survey acronym 'PESSTO' shall be used to refer to the combined PESSTO and ePESSTO surveys.

Table 1. PESSTO settings for EFOSC2 spectroscopy. The blocking filter OG530 is used only (and always) for Gr#16. The GG495 blocking filter is occasionally used from Gr#20. The 1" slit projects to 3.5 binned pixels. The column headed Arclines indicates the number of lines used. The RMS is the typical residual for the wavelength calibration solution.

Grism	Wavelength (Å)	Filter (blocking)	Dispersion (Åpix ⁻¹)	Resolution (Å for 1" slit)	Arclines (number)	RMS (Å)
#13	3650 - 9250	none	5.5	18.2	13-15	0.10-0.15
#11	3345 - 7470	none	4.1	13.8	9	0.10-0.15
#16	6000 - 9995	OG530	4.2	13.4	11-14	0.05-0.10
#18	4700-6770	none	1.0	7.6	7	0.01-0.08
#20	6047-7147	GG495	0.55	2.0	12	0.05-0.07

Table 2. PESSTO settings for SOFI spectroscopy. The 1" slit projects to 3.4 pixels FWHM, measured from arc lines. The column headed Arclines indicates the number of lines used. The RMS is the typical residual for the wavelength calibration solution. The order blocking filters used are 0.925μm (GBF) and 1.424μm (GRF) "cut-on" filters.

Grism	Wavelength (μm)	Filter (blocking)	Dispersion (Å pix ⁻¹)	Resolution (Å for 1" slit)	Arclines (number)	RMS (Å)
Blue	0.935 - 1.654	GBF	6.95	23	12-14	0.1-0.2
Red	1.497 - 2.536	GRF	10.2	33	7-8	0.2-0.5

Release Content

PESSTO observes single targets in long-slit mode and selects targets for two purposes as described in Smartt et al. (2015). The first is to classify targets as early as possible after discovery. PESSTO takes targets from many different public surveys which report their discoveries of transient sources. These "classification" spectra are taken with Grism#13 (and seldomly with Grism#11) and typically we aim for signal-to-noise in the continuum between 10-20 depending on the magnitude of the source. The main purpose is to reliably screen targets to determine their classification and redshift. The science goal of PESSTO (Smartt et al. 2015) is detailed follow-up and time series spectroscopic monitoring of supernovae at the extremes of the known population e.g. the most luminous, the faintest, the fast declining etc. Hence the screening classification spectra are necessarily kept short in order to minimize the time observing normal supernovae and maximize the time available for scientific follow-up.

In seven years, PESSTO has taken spectra of 2314 distinct objects. From this list, 306 supernovae (29 of which are super-luminous supernovae), 4 supernova imposters, 10 tidal disruption events, 8 unclassified objects, 2 AGN, 2 galactic novae, 3 variable stars, 1 FRB counterpart candidate and 1 kilonova were picked as interesting science targets and these were scheduled for follow-up time series EFOSC2 optical spectroscopy, with the brightest also having SOFI spectra. A

summary of these 337 PESSTO Key Science targets and the spectral data sets taken is given in Table 3. The total numbers of spectra released for these 337 "PESSTO Key Science" targets are 3406 EFOSC2 spectra and 342 SOFI spectra (a combined total of 3748). The EFOSC2 numbers includes any transient classification spectra taken.

PESSTO has used EFOSC2 in imaging mode to take acquisition images of many of the targets before a spectrum is taken and, in some cases, multi-colour photometry is taken. Smartt et al. (2015) describes the rationale for lightcurve construction for PESSTO science targets, which are typically bright enough to be done with smaller aperture facilities. SOFI imaging is nearly always taken when SOFI near infra-red spectra are taken. The higher resolution EFOSC grisms Gr#18 and Gr#20 were employed occasionally during the 2 years of ePESSTO, to allow higher spectral resolution for objects with H-Balmer lines in emission (see Table 1 for details of resolutions).

In total the SSDR4 contains 45.4 GB of data and the numbers of images and spectra are given in Table 4. In total there are 5560 EFOSC2 spectra released. These include the 3406 EFOSC2 spectra of Table 3. The remaining 2154 EFOSC spectra relate to 1977 objects for which we took spectra but did not pursue a detailed followup campaign. There are more spectra than objects simply due to the fact that in some cases PESSTO took more than one spectrum for classification due to either low signal-to-noise in the first spectrum, or ambiguous classifications that needed further spectra to allow a secure analysis. Generally, the first spectrum taken of an object was enough for a classification. However, there were circumstances in which further spectra were needed due to either low signal-to-noise, or a real ambiguity. The most common cause of ambiguity in classification are objects showing featureless blue continua. These are usually young type II SNe, but can be Galactic CVs, tidal disruption candidates, or moderate redshift superluminous supernovae. In these cases, further spectra usually show spectral features to allow redshift and classifications. The classifications released by PESSTO are based on the set of early spectra taken.

PESSTO has taken EFOSC2 images which include multi-colour follow-up images of science targets, EFOSC2 acquisition images, and standard star fields (fields are defined in Smartt et al. 2015). These EFOSC2 images will be astrometrically and photometrically calibrated (as far as the small field of view of EFOSC2 will allow). The raw images are available in the ESO archive and on www.pessto.org.

In some cases the astrometric position of the science target on SOFI (or the EFOSC2) images can be of order 0.5 – 1.5 arcsec different to that recorded in the headers of the 1D spectral files. The coordinates in the 1D spectral files are those of the target and these are taken from a range of surveys which can have minor, but measureable, errors in the absolute astrometry. The coordinates in the SOFI and EFOSC2 images are likely to be as good if not better than those originally provided from the feeder surveys, but discrepancies are typically less than 1.5 arcseconds.

In this release we also include the PESSTO Transient Catalogue, a catalogue of 2144 PESSTO sources for which a meaningful spectral classification has been obtained within the seven years of PESSTO operations.

Table 3: PESSTO SDR4 Key Science targets. These targets were selected for detailed follow-up in the seven years of survey operations, initially with EFOSC2 and with SOFI when possible. The numbers refer to the numbers of epochs of spectra taken with each Grism. Gr11, Gr13, Gr16, Gr18 and Gr20 refer to the EFOSC2 grisms and GB, GR refer to the SOFI grisms (GB = Blue and GR = Red, with details in Table 2).

Target	Type	Number of Spectra	Comments
ASASSN-14ha	SN II	14xGr11, 4xGr13, 13xGr16, 4xGB, 4xGR	
ASASSN-14hu	SN Ia	9xGr13	
ASASSN-14il	SN IIIn	4xGr11, 1xGr13, 4xGr16, 5xGB, 3xGR	
ASASSN-14ko	SN IIIn	4xGr11, 1xGr13, 4xGr16	
ASASSN-14kp	SN II	7xGr13	
ASASSN-14lp	SN Ia	8xGr11, 1xGr13, 8xGr16	
ASASSN-14lw	SN Ia-p	4xGr11, 4xGr16, 1xGB	
ASASSN-15be	SN Ia	2xGr11, 2xGr16	
ASASSN-15fz	SN II	2xGr11, 1xGr16	
ASASSN-15ga	SN Ia-p	3xGr11, 3xGr16, 2xGB, 2xGR	
ASASSN-15go	SN Ia	3xGr11, 3xGr16	
ASASSN-15hf	SN Ia	2xGr11, 1xGr13, 2xGr16	
ASASSN-15hx	SN Ia	1xGr11, 1xGr13, 1xGr16	
ASASSN-15hy	SN Ia-p	2xGr11, 1xGr13, 2xGr16	
ASASSN-15nr	SN Ia-p	1xGr11, 1xGr16	
ASASSN-15og	SN IIIn-p	7xGr11, 1xGr13, 7xGr16	
ASASSN-15oi	TDE	7xGr11, 5xGr13, 6xGr16, 1xGB	

ASASSN-15oz	SN II	7xGr13, 2xGB, 2xGR
ASASSN-15uo	SN II n-p	2xGr11, 1xGr13, 1xGr16
ASASSN-16kd	Galactic Nova	2xGr11, 2xGr16
ASASSN-18fv	Galactic Nova	53xGr11, 56xGr16, 55xGr18, 52xGr20, 10xGB, 10xGR
AT2015bm	SN II	11xGr13
AT2016bln	SN Ia	3xGr11, 2xGr13, 2xGr16
AT2016jbu	Impostor- SN	30xGr11, 1xGr13, 25xGr16
AT2017beq	SLSN I	2xGr11, 1xGr13, 1xGr16
AT2017egv	SN I	2xGr11, 1xGr13, 1xGr16
AT2017gfo	KN	3xGr11, 3xGr16, 1xGB
AT2017gge	unknown	8xGr13, 8xGr18, 1xGB
AT2017gpp	unknown	1xGr11, 6xGr13, 1xGr16
AT2017int	SN II	4xGr11, 3xGr13
AT2018bcb	AGN	3xGr11, 1xGr13, 3xGr16
AT2018buo	unknown	3xGr11, 1xGr13, 3xGr16
AT2018bwo	Variable Star	1xGr11, 1xGr16
AT2018dyb	TDE	9xGr11, 3xGr13, 7xGr16
AT2018fds	SN II	6xGr11, 7xGr13, 2xGr16
AT2018fyk	TDE	11xGr11, 4xGr13, 4xGr16
AT2018hyz	TDE	10xGr11, 8xGr16
AT2018lna	TDE	6xGr13
AT2018qb	unknown	2xGr11, 1xGr13, 1xGr16

AT2018ys	unknown	4xGr13	
AT2018zr	TDE	2xGr11, 2xGr16	
AT2019azh	TDE	1xGr11, 1xGr13, 1xGr16	
CSS121008-014245+213928	SN Ia	4xGr13	
CSS121015-004244+132827	SLSN II	16xGr13	Benetti et al. (2013)
CSS130403-150213+103846	SN Ia-p	7xGr11, 1xGr13, 3xGr16	
CSS130809-222004-213922	SN II	5xGr11, 3xGr13, 2xGr16	
CSS131031-095508+064831	SN Ia	1xGr11, 3xGr13, 1xGr16	
CSS131110-023957-083124	SN II	5xGr11, 4xGr13, 2xGr16	Gall et al. (2015)
CSS140421-142042+031602	SN Ibn	3xGr11, 9xGr13, 3xGr16	Hosseinzadeh et al. (2016)
CSS140424-133007-212728	SN IIn	6xGr11, 1xGr13, 1xGr16	
CSS140914-010107-101840	SN Ia	2xGr11, 2xGr13, 2xGr16	
CSS140925-005854+181322	SLSN Ic	4xGr13	
CSS150124-140455+085515	SN Ia	2xGr11, 2xGr16	
FRB180311	FRB	5xGr13, 2xGr18	
Gaia16aec	SN II	7xGr13	
Gaia16afe	SN Ia-p	2xGr13, 1xGB	
LSQ12btw	SN Ibn	1xGr11, 1xGr13, 1xGr16	Pastorello et al. (2015b)
LSQ12byu	SN Ia-p	4xGr13	
LSQ12dlf	SLSN Ic	1xGr11, 7xGr13, 1xGr16	Nicholl et al. (2014)
LSQ12dwl	SN Ic-p	2xGr11, 7xGr13, 2xGr16, 5xGB, 4xGR	
LSQ12dyw	SN Ic-p	1xGr11, 14xGr13, 1xGr16	
LSQ12fhs	SN Ia	3xGr11, 4xGr13	

LSQ12fxd	SN Ia	4xGr11, 1xGr13, 4xGr16	
LSQ12gdj	SN Ia	7xGr11, 7xGr16, 1xGB, 1xGR	Scalzo et al. (2013)
LSQ12gpw	SN Ia-p	4xGr11, 1xGr13, 4xGr16	
LSQ12gxb	SN I-p	3xGr11, 1xGr13, 1xGr16	
LSQ12hcm	SN II	1xGr11, 1xGr13, 1xGr16	
LSQ12heq	SN II n	4xGr11, 5xGr13, 2xGr16	
LSQ12hnj	SN II	1xGr11, 1xGr16	
LSQ12hot	SN II n	1xGr11, 9xGr13	
LSQ12hxg	SN II n	5xGr11, 8xGr13, 3xGr16	
LSQ13bnx	SN II	3xGr11, 1xGr13, 3xGr16	
LSQ13bvs	SN II	4xGr11, 4xGr16	
LSQ13ddu	SN I-p	4xGr11, 5xGr13, 3xGr16	
LSQ13deg	AGN	5xGr13	
LSQ13fn	SN II n	13xGr11, 9xGr13, 6xGr16	Polshaw et al. (2016)
LSQ13sj	SN II	7xGr13	
LSQ14abd	SN Ia	2xGr11, 1xGr13, 3xGr16	
LSQ14an	SLSN Ic	9xGr11, 9xGr13, 9xGr16	
LSQ14asn	SN II	8xGr11, 3xGr13	
LSQ14bdq	SLSN Ic Variable	1xGr11, 3xGr13	Nicholl et al. (2015)
LSQ14bjb	Star	1xGr13, 1xGr16	
LSQ14eer	SN II	4xGr11, 1xGr13	
LSQ14eez	SN I	7xGr13	
LSQ14efd	SN I	2xGr11, 14xGr13	
LSQ14fxj	SLSN Ic	2xGr11, 7xGr13, 2xGr16	
LSQ14gfb	SN Ia-p	2xGr11, 4xGr13, 2xGr16	

LSQ14gqk	SN Ibc	1xGr11, 7xGr13, 1xGr16, 1xGB	
LSQ14ii	unknown	4xGr13	
LSQ14mo	SLSN Ic	5xGr11, 14xGr13, 3xGr16	
LSQ14nr	SN Ia	1xGr11, 3xGr13, 1xGr16	
LSQ14pt	SN IIn	5xGr11, 1xGr13, 11xGr16	
LSQ15abl	SLSN II	3xGr11, 1xGr13, 2xGr16	
LSQ15adm	SN Ia-p	11xGr11, 2xGr13, 8xGr16, 2xGB, 2xGR	
LSQ15bfp	SN Ic-p	5xGr13	
LSQ15kp	SN II	5xGr11, 10xGr13, 5xGr16	
LSQ15rw	SN IIb	7xGr13	
MAS- TERJ003918.04+035659.6	SN Ia	3xGr11, 1xGr13, 3xGr16, 1xGB, 1xGR	
MASTERJ141023.42- 431843.7	SN Ib	7xGr13	
NGC7552-OT	Impostor- SN	6xGr11, 7xGr16	
NGC772-OT1	Impostor- SN	1xGr13, 7xGr16, 1xGB	
OGLE-2012-SN-006	SN Ibn	1xGr11, 6xGr13, 1xGr16, 2xGB, 2xGR	Pastorello et al. (2015b)
OGLE-2012-SN-040	SN Ia	3xGr11, 3xGr13, 3xGr16, 1xGB, 1xGR	
OGLE-2013-SN-016	SN IIn	9xGr11, 1xGr13, 7xGr16	
OGLE-2013-SN-019	SN IIP	4xGr11, 1xGr13	
OGLE-2013-SN-079	SN I	4xGr11, 4xGr13, 2xGr16	Inserra et al. (2015)
OGLE-2013-SN-100	SN II-p	8xGr13, 1xGr16	
OGLE-2013-SN-118	SN Ia	3xGr11, 2xGr13, 2xGr16	
OGLE-2014-SN-012	unknown	2xGr11, 3xGr13	

OGLE-2014-SN-047	SN Ic	8xGr13	
OGLE-2014-SN-073	SN II	14xGr13	
OGLE-2014-SN-122	SN IIn	2xGr13, 1xGr16	
OGLE-2014-SN-131	SN Ibn	2xGr11, 1xGr13, 1xGr16	
OGLE-2014-SN-189	unknown	3xGr11, 1xGr13	
OGLE-2015-SN-035	SN II	1xGr11, 13xGr13, 1xGr16	
OGLE-2015-SN-043	SN II	4xGr13	
OGLE-2015-SN-065	SN IIn	1xGr11, 1xGr13, 1xGr16	
OGLE15qz	SLSN Ic	3xGr11, 2xGr13, 3xGr16	
OGLE15sd	SLSN Ic	5xGr11, 1xGr13	
OGLE15xl	SLSN Ic	2xGr11, 16xGr13, 2xGr16	
OGLE16aaa	TDE	9xGr13	Wyrzykowski et al. (2016)
OGLE16dmu	SLSN I	11xGr11, 10xGr13, 7xGr16	
OGLE16eun	SN Ibc	1xGr11, 1xGr13, 1xGr16	
OGLE16euo	SN Ia	3xGr11, 4xGr13, 5xGr16	
OGLE17aaj	TDE	3xGr11	
PS15ae	SLSN Ic	5xGr11, 4xGr13, 5xGr16, 4xGB, 1xGR	Nicholl et al. (2016a, 2016b), Jerkstrand et al. (2016)
PS15br	SLSN Ic	4xGr11, 16xGr13, 4xGr16	Inserra et al. (2016)
PS15cwo	SN II	7xGr11, 1xGr13, 7xGr16	
PS15cww	SN IIn	8xGr11, 8xGr13, 2xGr16, 1xGB	
PS15cwz	SN Ia	1xGr11, 1xGr16	
PS15cwz	SN Ia	4xGr11, 2xGr13, 4xGr16	
PS15dpn	SN II	2xGr11, 2xGr13, 2xGr16	

PS15dsr	SN II	2xGr11, 3xGr13, 2xGr16	
PS15yr	SN IIb	3xGr11, 3xGr16	
PSNJ09204691-0803340	SN IIIn	8xGr11, 6xGr16	
PSNJ11484578-2817312	SN Ic	1xGr11, 1xGr13, 1xGr16	
PSNJ14095513+1731556	SN Ia	1xGr11, 3xGr13, 1xGr16	
PSNJ15053007+0138024	SN Ia-p	7xGr13, 3xGB, 2xGR	
PSNJ15213475-0722183	Impostor- SN	6xGr11, 1xGr13, 2xGr16	
PSNJ21505094-7020289	SN Ia	1xGr11, 1xGr16	
SN2006sa	SN IIP	5xGr13	
SN2009ip	SN IIIn-p	27xGr11, 5xGr13, 21xGr16, 8xGB, 6xGR	Fraser et al. (2013), Fraser et al. (2015)
SN2012ca	SN IIIn	18xGr13, 5xGB, 3xGR	Inserra et al. (2013, 2016)
SN2012dy	SN II	12xGr11, 6xGr13, 9xGr16	
SN2012ec	SN IIP	14xGr11, 2xGr13, 11xGr16, 11xGB, 4xGR	Maund et al. (2013), Barbarino et al. (2015), Jerkstrand et al. (2015)
SN2012fr	SN Ia	15xGr11, 2xGr13, 15xGr16, 10xGB, 9xGR	Childress et al. (2013), Childress et al (2015)
SN2012hd	SN Ia	2xGr11, 1xGr13, 2xGr16	Maguire et al. (2013)
SN2012hn	SN Ic-p	3xGr11, 1xGr13, 3xGr16	Valenti et al. (2013)
SN2012hr	SN Ia	3xGr11, 1xGr13, 3xGr16, 2xGB, 1xGR	Maguire et al. (2013)
SN2012hs	SN IIb	7xGr11, 7xGr13, 7xGr16, 3xGB, 1xGR	

SN2012ht	SN Ia	3xGr11, 3xGr16, 2xGB, 1xGR	Maguire et al. (2013)
SN2013K	SN IIP	6xGr11, 18xGr13, 7xGr16, 1xGB	
SN2013U	SN Ia-p	3xGr11, 3xGr16	Maguire et al. (2013)
SN2013ai	SN II	3xGr11, 11xGr13	
SN2013aj	SN Ia	3xGr11, 2xGr13, 3xGr16	Maguire et al. (2013)
SN2013ak	SN II	8xGr11, 6xGr16, 3xGB, 3xGR	
SN2013am	SN II	7xGr13, 3xGB, 3xGR	
SN2013ao	SN Ia	11xGr11, 1xGr13, 9xGr16	Maguire et al. (2013)
SN2013bb	SN IIb	4xGr11, 6xGr13, 4xGr16	
SN2013dn	SN IIIn	3xGr11, 5xGr13, 3xGr16	
SN2013ej	SN II	13xGr11, 2xGr13, 13xGr16, 5xGB, 5xGR	Yuan et al. (2016)
SN2013ek	SN Ic	5xGr11, 1xGr13, 5xGr16, 2xGB	
SN2013ew	SN Ia-p	7xGr11, 2xGr13, 7xGr16	
SN2013fc	SN IIIn	9xGr11, 7xGr13, 6xGr16, 2xGB, 2xGR	Kangas et al. (2016)
SN2013fq	SN IIb	4xGr11, 1xGr13, 4xGr16, 1xGB, 1xGR	
SN2013fs	SN IIP	8xGr11, 6xGr16, 1xGB, 1xGR	
SN2013gr	SN Ia-p	11xGr11, 5xGr13, 10xGr16	
SN2013hx	SLSN II	4xGr11, 3xGr13, 4xGr16	Inserra et al. (2016)
SN2014L	SN Ic	3xGr11, 3xGr16	
SN2014ad	SN Ic	2xGr11, 3xGr13, 2xGr16	

SN2014cx	SN II	7xGr11, 13xGr13, 7xGr16, 5xGB, 4xGR	
SN2014dq	SN IIP	3xGr11, 4xGr13, 4xGB	
SN2014eg	SN Ia	12xGr11, 1xGr13, 10xGr16, 2xGB, 1xGR	
SN2015D	SN II	11xGr11, 1xGr13, 8xGr16	
SN2015F	SN Ia	12xGr11, 1xGr13, 11xGr16, 9xGB, 9xGR	
SN2015H	SN Ia-p	5xGr11, 6xGr13, 5xGr16, 3xGB, 1xGR	Magee et al. (2016)
SN2015L	TDE	15xGr11, 5xGr13, 15xGr16	
SN2015ah	SN Ib	4xGr11, 4xGr16, 1xGB, 1xGR	
SN2015ap	SN Ib	5xGr11, 3xGr16, 1xGB, 1xGR	
SN2015ay	SN II	5xGr13	
SN2016B	SN IIP	10xGr13, 3xGB, 3xGR	
SN2016O	SN IIP	8xGr13	
SN2016P	SN Ic-p	6xGr11, 6xGr16	
SN2016X	SN IIP	4xGr11, 4xGr16, 2xGB, 2xGR	
SN2016adj	SN Ib	5xGr11, 6xGr16, 7xGB, 7xGR	
SN2016ado	SN Ia	1xGr11, 1xGr13, 1xGr16	
SN2016aiy	SN IIIn	6xGr11, 2xGr13, 6xGr16	
SN2016aj	SLSN Ic	4xGr13	
SN2016aqf	SN IIP	15xGr13	
SN2016blz	SN II	5xGr11, 2xGr13, 5xGr16	
SN2016cvk	SN IIIn-pec	11xGr11, 10xGr16, 3xGB, 3xGR	

SN2016egz	SN II	2xGr11, 13xGr13
SN2016eiy	SN Ia	2xGr11, 2xGr13, 2xGr16
SN2016els	SLSN-I	4xGr11, 3xGr16
SN2016enp	SN II	4xGr11, 5xGr13, 3xGr16
SN2016eso	SN II _n	1xGr11, 1xGr16
SN2016ezh	SN II	10xGr11, 1xGr13, 10xGr16, 2xGr18, 1xGB, 1xGR
SN2016fmb	SN Ia	2xGr11, 1xGr13, 2xGr16
SN2016frp	SN Ib-p	3xGr11, 3xGr13, 3xGr16
SN2016geu	SN Ia	4xGr13
SN2016gkg	SN II _b	13xGr11, 12xGr16, 5xGB, 4xGR
SN2016gsd	SN II	4xGr13
SN2016hmq	SN II	10xGr13
SN2016hnk	SN Ia	4xGr11, 13xGr13, 4xGr16, 1xGB
SN2016hvl	SN Ia	5xGr11, 5xGr13, 5xGr16
SN2016iae	SN Ic	6xGr11, 4xGr13, 7xGr16
SN2016ija	SN II	2xGr11, 10xGr16, 5xGB, 4xGR
SN2016ije	SN Ia	2xGr11, 7xGr13, 2xGr16, 1xGB, 1xGR
SN2016iks	SN Ia	7xGr11, 1xGr13, 6xGr16
SN2016ipf	SN Ia	3xGr11, 3xGr16
SN2016iyd	SN II	11xGr11, 1xGr13, 1xGr16
SN2017abw	SN II	3xGr11, 1xGr13, 2xGr16
SN2017aww	SN II	5xGr13
SN2017awz	SN Ia	5xGr11, 3xGr13, 5xGr16

SN2017azw	SN Ia	2xGr11, 1xGr13, 2xGr16
SN2017bkc	SN Ia	1xGr11, 3xGr13, 1xGr16
SN2017bzc	SN Ia	4xGr11, 3xGr13, 4xGr16
SN2017cbv	SN Ia	4xGr11, 4xGr13, 4xGr16, 3xGB, 3xGR
SN2017cfo	SN II	5xGr13
SN2017cfq	SN	2xGr11, 2xGr16
SN2017cik	SN II _n	1xGr11, 1xGr16
SN2017cjb	SN II	1xGr11, 1xGr16
SN2017ckq	SN Ia	1xGr11, 3xGr13, 1xGr16
SN2017cyy	SN Ia	2xGr11, 3xGr13, 2xGr16
SN2017dcc	SN Ic	4xGr11, 1xGr13, 4xGr16
SN2017dfb	SN Ia	3xGr11, 3xGr16
SN2017dft	SN Ia	6xGr13
SN2017dht	SN II-p	1xGr11, 2xGr13, 1xGr16
SN2017dio	SN Ic	2xGr11, 1xGr13, 2xGr16
SN2017dka	SN II	1xGr11, 1xGr13, 1xGr16
SN2017eby	SN Ia	2xGr11, 1xGr13, 2xGr16
SN2017ejb	SN Ia	1xGr11, 1xGr16
SN2017ens	SLSN I	7xGr11, 2xGr13, 8xGr16
SN2017fwm	SN Ic	6xGr13
SN2017fzw	SN Ia	12xGr11, 6xGr13, 12xGr16, 9xGB
SN2017gah	SN Ia	14xGr11, 13xGr16, 4xGB
SN2017gax	SN Ibc	7xGr11, 7xGr16, 3xGB, 1xGR
SN2017gci	SLSN I	11xGr13

SN2017gga	SN II	1xGr11, 6xGr13, 1xGr16
SN2017gir	SN II n	1xGr11, 4xGr13, 1xGr16
SN2017gmr	SN II	2xGr11, 2xGr16, 3xGB, 3xGR
SN2017guh	SN Ia	2xGr11, 2xGr16
SN2017gvp	SN Ia	2xGr11, 2xGr16
SN2017hbj	SN II	8xGr13
SN2017hcc	SN II n	5xGr11, 5xGr16, 3xGB, 3xGR
SN2017hm	SN Ia	3xGr11, 3xGr13, 3xGr16
SN2017hn	SN Ia	4xGr11, 1xGr13, 4xGr16
SN2017hpi	SN II	14xGr13
SN2017hrq	SN II	3xGr11, 1xGr13, 3xGr16, 1xGr20
SN2017htp	SN Ic	4xGr13
SN2017hxz	SN II	2xGr11, 4xGr13, 1xGr16
SN2017hya	SN Ia	3xGr11, 1xGr13, 3xGr16
SN2017ifu	SN Ia	3xGr11, 4xGr13, 2xGr16
SN2017ijn	SN II n	11xGr11, 10xGr16, 2xGB, 1xGR
SN2017imj	SN II	1xGr11, 3xGr13
SN2017iue	SN II	1xGr11, 3xGr13
SN2017iuk	SN Ic	10xGr11, 3xGr13, 10xGr16, 1xGB, 1xGR
SN2017ivv	SN II	12xGr13
SN2017jan	SLSN I	2xGr11, 3xGr13, 2xGr16
SN2017jei	SN II	7xGr11, 1xGr13, 6xGr16
SN2017jfs	SN II n	4xGr11, 1xGr13
SN2017jfv	SN Ibn	2xGr11, 1xGr13, 1xGr16
SN2017pn	SN II	5xGr13

SN2017vp	SN II	4xGr13
SN2017yv	SN Ia	2xGr11, 4xGr13, 2xGr16
SN2018aad	SN II-p	6xGr11, 5xGr16
SN2018agk	SN Ia	3xGr11, 3xGr16
SN2018ahq	SN Ia	1xGr11, 4xGr13, 1xGr16
SN2018aoz	SN Ia	2xGr11, 1xGr13, 2xGr16
SN2018apo	SN Ia	1xGr11, 2xGr13, 1xGr16
SN2018atq	SLSN II	2xGr11, 7xGr13, 2xGr16
SN2018beh	SN Ib	2xGr11, 2xGr13, 2xGr16
SN2018bgz	SN Ia	1xGr11, 1xGr13, 1xGr16
SN2018bie	SN Ia	1xGr11, 1xGr13, 1xGr16
SN2018bsz	SN II	6xGr11, 3xGr13, 5xGr16
SN2018cnf	SN II n	3xGr11
SN2018coq	SN II	5xGr13
SN2018ec	SN Ic	7xGr13, 3xGB
SN2018emt	SN II	1xGr11, 4xGr13
SN2018enc	SN Ia	2xGr13, 1xGB
SN2018eov	SN Ia	2xGr13, 2xGB
SN2018eph	SN II	2xGr11, 7xGr13, 3xGr16
SN2018evy	SN II	2xGr11, 2xGr13, 2xGr16
SN2018exb	SN Ia	1xGr13, 2xGB
SN2018exc	SN Ia	2xGr13, 2xGB
SN2018fcg	SLSN I	1xGr11, 1xGr13, 1xGr16
SN2018ffj	SLSN I	4xGr11, 2xGr13, 7xGr16
SN2018fit	SN II	7xGr13
SN2018fus	SN II	1xGr11, 5xGr13
SN2018fvx	SN II	3xGr11, 1xGr13

SN2018gft	SLSN I	3xGr11, 1xGr13, 3xGr16
SN2018ghb	SN Ia	1xGr11, 2xGr13, 1xGr16
SN2018giu	SN Ic	3xGr11, 1xGr13, 3xGr16
SN2018gjx	SN IIb	3xGr11, 4xGr13, 1xGr16
SN2018gl	SN Ia	3xGr11, 2xGr16
SN2018gsk	SN Ic	4xGr11, 4xGr13, 4xGr16
SN2018hfm	SN II	5xGr13, 1xGB
SN2018hfp	SN Ia	1xGr13, 1xGB
SN2018hgc	SN Ia	2xGr13, 1xGB
SN2018hhn	SN Ia	1xGr11, 1xGr16, 2xGB
SN2018hjwt	SN Ia	2xGr13, 1xGB
SN2018hjt	SN Ib	1xGr11, 4xGr13, 1xGr16
SN2018hti	SLSN I	5xGr11, 2xGr13, 5xGr16
SN2018htt	SN Ia	1xGr11, 1xGr16
SN2018ibb	SLSN I	3xGr11, 2xGr13, 3xGr16
SN2018ilu	SN Ia	1xGr11, 3xGr13, 1xGr16
SN2018iuq	SN II	9xGr13
SN2018ivc	SN II	2xGr11, 2xGr13, 2xGr16
SN2018jtz	SN II	1xGr11, 7xGr13
SN2018jkb	SN II	3xGr11, 1xGr13, 3xGr16
SN2018jky	SN Ia	1xGr13, 1xGB
SN2018jmt	SN Ibn	2xGr11, 2xGr13, 1xGr16
SN2018khh	SN II n	3xGr11
SN2018kpo	SN II	2xGr11, 3xGr13, 2xGr16
SN2018kzr	SN Ic	2xGr11, 3xGr13, 2xGr16
SN2018ldu	SN II	6xGr13

SN2018lfe	SLSN I	2xGr11, 2xGr13, 2xGr16	
SN2018oh	SN Ia	9xGr11, 1xGr13, 6xGr16, 3xGB	
SN2018rw	SN Ia	3xGr11, 8xGr13, 3xGr16	
SN2018yu	SN Ia	3xGr11, 3xGr16	
SN2019abu	SN II	4xGr13	
SN2019akg	SN Ia	2xGr13, 1xGB	
SN2019ape	SN Ic	1xGr11, 2xGr13, 1xGr16	
SN2019asz	SN II	2xGr11, 2xGr13	
SN2019awq	SN Ia	1xGr13, 1xGB	
SN2019bao	SN IIb	2xGr11, 1xGr16	
SN2019bdz	SN Ia	2xGr13, 1xGB	
SN2019bka	SN Ia	2xGr11, 2xGr16	
SN2019bkc	SN Ic-p	1xGr11, 1xGr13, 1xGr16	
SN2019cj	SN Ibn	4xGr11, 2xGr13	
SN2019rm	SN Ia	5xGr13	
SN2019so	SN Ia	5xGr11, 1xGr13, 4xGr16	
SSS120810-231802- 560926	SLSN Ic	12xGr13	Nicholl et al. (2014)
SSS130221-133330- 194457	SN IIc	7xGr11, 6xGr13	
SSS130404-102043- 062657	SN Ia	2xGr11, 3xGr13, 2xGr16	
TCPJ17344775-2409042	Variable star	1xGr11, 1xGr16	
iPTF13dge	SN Ia	4xGr11, 4xGr16	

Table 4: Total number of science files released in the various formats described here.

File Type	Format	Number of Files	Data Volume
EFOSC2 1D spectra	Binary table	5560	0.3 GB
EFOSC2 2D spectral images	FITS image	5560	19.1 GB
SOFI 1D spectra	Binary table	342	0.02 GB
SOFI 2D spectral images	FITS image	342	1.3 GB

SOFI images	FITS image	1580	12.4 GB
SOFI image weights	FITS image	1580	12.4 GB
TOTAL		14964	45.4 GB

Release Notes

Data Reduction, Calibration and Quality

1. EFOSC2 Spectroscopic calibration data and reduction

Bias calibration: A set of 11 bias frames are typically taken each afternoon of PESSTO EFOSC2 observations and are used to create a nightly master bias. This nightly master bias frame is applied to all EFOSC2 data taken, including the spectroscopic frames, the acquisition images and any photometric imaging. The frame used for the bias subtraction can be tracked in the header keyword.

```
ZEROCOR = 'bias_20130402_Gr11_Free_56448.fits'
```

The file name gives the date the bias frames were taken, the Grism and filter combinations for which it is applicable (of course for biases this is not relevant but the pipeline keeps track with this nomenclature) and the MJD of when the master bias was created. The dark current is less than $3.5 \text{ e}^- \text{ pix}^{-1} \text{ hr}^{-1}$, hence with typical PESSTO exposures being 600-1800s, no dark frame correction is made.

Flat field calibration : The PESSTO survey takes sets of spectroscopic flatfields in the afternoons at a typical frequency of once per sub-run of 3-4 nights. Five exposures are taken with maximum count levels of 40,000-50,000 ADU for each of the grism, order sorting filter, and slit width combinations that we use (8 combinations in total). Each of these is combined to give a masterflat which can be associated with the appropriate science observations from the sub-run.

```
FLATCOR = 'nflat_20130413_Gr11_Free_slit1.0_100325221_56448.fits'
```

The EFOSC2 CCD#40 is a thinned chip, hence has significant fringing beyond 7200\AA and the severity depends upon the grating used. The only way to remove fringing (in spectroscopic mode) is to take a calibration flat field lamp exposure immediately after or before the science image and use this to divide into the science spectrum. PESSTO always takes internal lamp flats (3 exposures of typically 40,000 ADU maximum count level) after taking any science spectra with Gr#16. More details on the exact methods used are given in Smartt et al. (2015).

Cosmic ray removal : The PESSTO pipeline incorporates a modified version of the python implementation of LaCOSMIC (Van Dokkum 2001) to remove cosmic rays in the central 200 pixels around the object (i.e. central pixel ± 100 pixels).

Arc frames and wavelength calibrations: Arc frames are taken in the evening before observing and in the morning after the night finishes. EFOSC2 has helium and argon lamps and PESSTO uses both of these lamps turned on together. No arc frames

are taken during the night to reduce overheads. Although EFOSC2 suffers from significant flexure as the instrument rotates at the nasmyth focus (which can be 4 pixels over 200 degrees in rotation), the flexure causes a rigid shift of the wavelength frame. Hence we apply the calibration determined from the evening arc frames and adjust this with a linear offset as measured from either the skylines or atmospheric absorption lines. Relatively high order Legendre polynomial fits (5-6) are needed to fit the EFOSC2 arc lines with a fit which produces no systematic residuals. The number of arc lines used for the dispersion solution of each object, along with the RMS error, are given in the header of the reduced spectra by the keywords LAMNLIN and LAMRMS respectively. The formal RMS values are probably too small to realistically represent the uncertainty in the wavelength calibration at any particular point, given the FWHM of the arclines is 13-17Å. Hence this might suggest over-fitting of the sampled points. As a comparison, Legendre polynomials with order 4 produced obvious systematic residuals and RMS values of between 0.4-1.0Å for a 1.0" slit and 1-1.8Å for a 1."5 slit. For exposures longer than 300 s, the linear shift applied to the dispersion solution is measured from the night sky emission lines. For shorter exposures such as spectrophotometric standards, the night sky lines are not visible, and the shift is instead measured from the telluric absorptions in the extracted 1D spectrum. The linear shifts are typically in the range of 6-13 Å for Gr#11 and Gr#13. In the case of Gr#16 spectra the shifts were usually smaller, usually 4-9 Å. This value of linear shift is recorded in the header keyword SHIFT. The linear shifts are calculated by cross-correlating the observed spectrum (sky or standard) with a series of library restframe spectra which are off set by 0.1Å. The library spectrum which produces the minimum in the cross-correlation function is taken as the correct match and this shift is applied. This method limits the precision of the shift to 0.1Å, which is roughly 1/40 of a pixel and less than 1/100 of a resolution element. This value of 0.1Å is recorded in the header as the systematic error in the wavelength calibration (SPEC_SYE). For all EFOSC2 spectra the wavelength axis reports wavelengths as measured in dry air.

Spectrophotometric standards and flux calibration: PESSTO uses a set of 9 spectrophotometric standard stars for (see Smartt et al. 2015) and we typically observe an EFOSC2 spectrophotometric standard three times per night (start, middle and end), although if there are significant SOFI observations or weather intervenes then this may be reduced. Generally, the three observations will include 2 different stars and a set of observations is taken with all grism, slit and filter combinations used during the nights observing. To remove any second order contamination in the flux standards, PESSTO always takes Gr#13 data for these stars with and without the filter GG495, to allow correction for the effect during pipeline reductions. Flux standards are always observed unless clouds, wind or humidity force unexpected dome closure. Hence even during nights which are not photometric, flux standards are taken and the spectra are flux calibrated; we deal with the issue of the absolute flux reliability below. A sensitivity function is derived for each EFOSC2 configuration from the spectrophotometric standards observed for each night. This was then applied to the final reduced spectra. In a few instances, a sensitivity curve was not created for a particular configuration on a given night, as there were no appropriate standards observed. In these cases, the sensitivity function from the preceding or following night was used.

The standard method of ensuring spectra are properly flux calibrated is to compare synthetic photometry of the science spectra with contemporaneous calibrated photometry and apply either a constant, linear or quadratic multiplicative function to the spectra to bring the synthetic spectra into line with the photometry. For PESSTO SDR1 this is not yet possible for all spectra since the photometric lightcurves are not yet finalised for many of the science targets and the classification spectra do not have a photometric sequence. However it is useful to know what the typical uncertainty is in any flux calibrated PESSTO spectrum, and this is encoded in the header keyword FLUXERR. PESSTO observes through non-photometric nights, and during these nights all targets are still flux calibrated. Hence the uncertainties in flux calibrations come from transparency (clouds), seeing variations that cause mismatches between sensitivity curves derived using standards with different image quality, and target slit positioning. Finally, photometric flux is generally measured with point-spread-function fitting which inherently includes an aperture correction to determine the total flux whereas spectroscopic flux is typically extracted down to 10 per cent of the peak flux (a standard practice in IRAF's `apall` task). All of this means that large percentage variations are expected and we carried out tests as to how well this method works and what is the reliability of the absolute flux calibration in the spectra. In Smartt et al. (2015) we describe these quantitative tests, and we have used the photometric sequence of SN2013ej to test this 2nd years data release (Yuan et al., in prep). This is illustrated in Fig. 1. We find that the RMS scatter in the absolute spectroscopic flux calibration is 36% and this is recorded in the headers of all spectra.

FLUXERR = 36 /Fractional uncertainty of the flux [%]

Science users should use this as a typical guide, if the seeing (as can be measured on the 2D frames and acquisition images) and night conditions (from the PESSTO wiki night reports; see Smartt et al. 2015) are reasonable. In future data releases we plan to significantly improve on the flux calibration scatter by using flux calibrated acquisition images.

Telluric absorption correction: PESSTO uses a model of the atmospheric absorption to correct for the H₂O and O₂ absorption (see Smartt et al. 2015 for details). This is carried out for all grism setups. The intensities of H₂O and O₂ absorptions in the atmospheric absorption model are first Gaussian smoothed to the nominal resolution of each instrumental setup, and then rebinned to the appropriate pixel dispersion. The pipeline then scales the model spectrum so that the intensities of H₂O and O₂ absorptions match those observed in the spectrophotometric standards, hence creating multiple model telluric spectra per night. Each science spectrum is then corrected for telluric absorption, by dividing it by the smoothed, rebinned, and scaled absorption model which is most closely matched in time i.e. closest match between the standard star observation time and the science observation time.

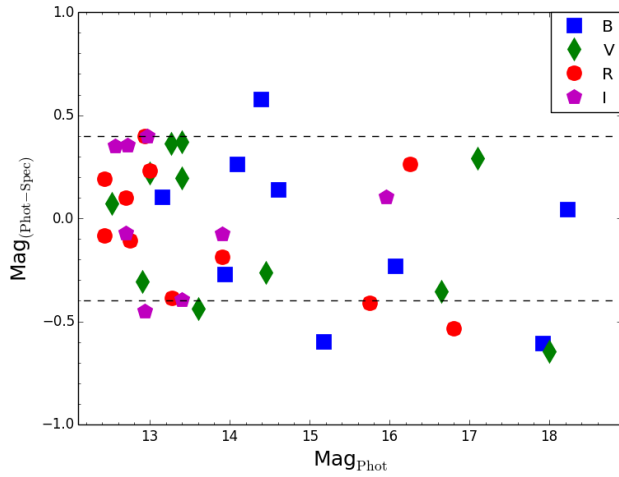


Fig 1: Synthetic magnitudes as measured from flux-calibrated spectra (Gr#11 and Gr#16) compared to the photometric magnitude at the same epoch for SN2013ej (Yuan et al. 2016.). Mag_{Phot} is the calibrated photometric magnitude and the y-axis is the difference between this and the synthetic photometry measured from the flux calibrated spectra. Colours and symbols indicate filters. The mean of all the values is -0.058 with a RMS of 0.360 .

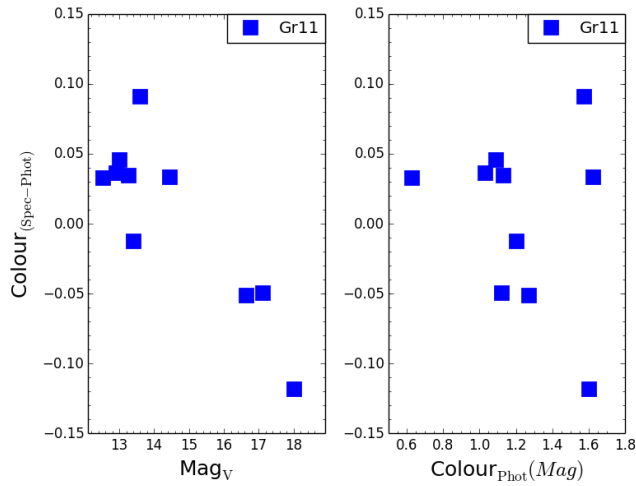


Fig 2: A check on the relative flux calibration of the PESSTO spectra. The difference between the synthetic photometry colours of SN2013ej (Gr#11) and photometric measurements is plotted on the y-axis. The x-axis is simply the V -band photometric magnitude on the left panel and photometric colour $B - V$ on the right. The colour RMS is 0.058 .

2. SOFI Spectroscopic calibration data and reduction

Similar to PESSTO observations and reductions for EFOSC2, we aim to homogenise the SOFI observations and calibrations and tie them directly to what is required in the data reduction pipeline. A standard set of PESSTO OB for calibrations and science are available on the PESSTO wiki and the following sections describe how they are applied in the pipeline reduction process. An example of a fully calibrated SOFI spectrum illustrating the wavelength range and atmospheric windows is shown in Fig. 2.

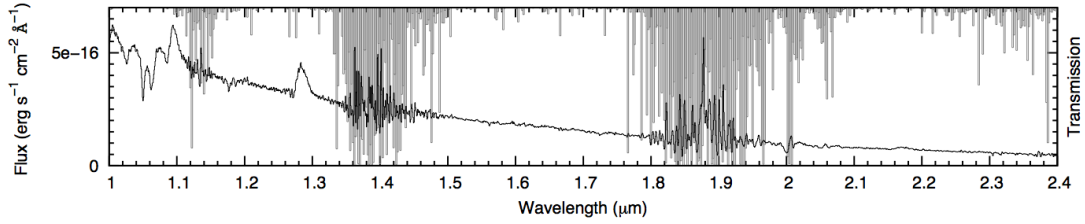


Fig 2. Combined blue and red grism SOFI spectra of SN 2012ec taken on 2013 September 24. Overplotted in grey is the atmospheric transmission, showing the correspondence between regions of low transparency and poor S/N in the spectrum.

Bias, dark and cross-talk correction: The detector bias offset and structure is subtracted along with the sky background, as is standard procedure with this chip. The SOFI detector suffers from cross talk, where a bright source on either of the two upper or lower quadrants of the detector will be accompanied by a “ghost” on the corresponding row on the opposite two quadrants. This cross-talk effect is corrected for within the PESSTO pipeline by summing each row on the detector, scaling by a constant value, and subtracting from the opposite quadrants.

Flat field calibration: The lamp-off flats are subtracted from the lamp-on flats, to remove the thermal background of the system. These subtracted flat fields are combined and normalized and used to correct for the pixel to pixel variations in detector sensitivity in the science and standard star frames. The amplitude of the variability in the flat field is $\sim 4\%$ for the red grism and $\sim 6\%$ for the blue grism. Two normalized red grism flat fields taken ~ 5 months apart show exactly the same structure, demonstrating that the flat field is stable, and that the use of monthly calibrations is justified (see Smartt et al. 2015).

Arc frames and wavelength calibrations : wavelength calibration is performed using spectra of a Xenon arc lamp. To fit the dispersion solution of the arc spectra without any systematic residuals requires a 4th order polynomial fit (see Table 2 for details of numbers of lines and RMS). This dispersion solution is applied to the two dimensional spectra and the sky lines are cross-correlated with an accurately calibrated template sky. A linear shift is applied to the wavelength calibration and recorded in the header keyword SHIFT. As with the EFOSC2 correction, the precision of the wavelength correction is limited to 0.1\AA , due to the scale of the shifts in the library sky spectra employed. Hence this value of 0.1\AA , is again recorded as the systematic error in the wavelength calibration (SPEC_SYE). As with EFOSC2 spectra, for all SOFI spectra the wavelength axis reports wavelengths as measured in dry air.

Sky subtraction and spectral extraction : SOFI spectra for PESSTO are taken in an ABBA dither pattern. This pattern consists of taking a first (A_1) exposure at a position ‘A’, then moving the telescope so that the target is shifted along the slit of SOFI by ~ 5 - $10''$ to position ‘B’. Two exposures are taken at ‘B’ (B_1 and B_2), before the telescope is offset back to ‘A’ where a final exposure (A_2) is taken. The pipeline subtracts each pair of observations (i.e, $A_1 - B_1$, $B_1 - A_1$, $B_2 - A_2$, $A_2 - B_2$) to give individual bias- and sky-subtracted frames and shifts these sky-subtracted frames so that the trace of

the target is at a constant pixel position, and the frames are then combined. Finally, the spectrum is optimally extracted interactively.

Telluric absorption correction : A “telluric standard” is observed immediately prior to or following the science spectrum, and at a similar airmass. The spectrum of the telluric standard is then divided by an appropriate template spectrum of the same spectral type, yielding an absorption spectrum for the telluric features. The absorption spectrum is then divided into the science spectrum to correct for the telluric absorption. As part of PESSTO, we observe either a Vega-like (spectral type A0V) or a Solar analog (G2V) telluric standard for each SOFI spectrum. The PESSTO pipeline uses the closest (in time) observed telluric standard to each science or standard star spectrum.

Spectrophotometric standards and flux calibration : The process for correcting the spectrum for the telluric absorption also provides a means for flux calibration using the Hipparcos I or V photometry of the solar analogs and Vega standards used. The flux of the observed telluric standard spectrum is scaled to match the tabulated photometry, with the assumption that the telluric standards have the same color (temperature) as Vega or the Sun. A second step is performed to flux calibrate the spectra using a spectrophotometric standard. The spectrophotometric standard is reduced and corrected for telluric absorption using a telluric standard, with the same technique as used for the science targets. This corrected standard spectrum is then compared with its tabulated flux, and the science frame is then linearly scaled in flux to correct for any flux discrepancy. There are only a handful of spectrophotometric standard stars which have tabulated fluxes extending out as far as the K-band (listed in Table 2 of Smartt et al. 2015). All SOFI spectra have the following keyword which denotes which telluric standard was used for both the telluric correction and the initial flux calibration.

```
SENSFUN = 'Hip105672_20130816_GB_merge_57000_1_ex.fits' /tell stand frame
```

The spectrophotometric flux standard from Smartt et al. (2015; Table 3) used to additionally scale the flux and the keyword `SENSPHOT` is added to the header, with the spectrum used to apply the flux calibration. This file has the name of the standard labelled.

```
SENSPHOT= 'sens_Feige110_20130816_GB_merge_57000_1_f.fits' / sens used to flux cal
```

To improve the scaling of the absolute flux levels of the spectra, we employ the *JHKs* imaging that is normally done when SOFI spectra are taken. Synthetic *J* and *H*-band photometry was performed on the blue grism spectra, and *H* and *K*-band photometry on the red grism spectra. The magnitude offsets between the *JHK* synthetic photometry and the *JHK* aperture photometry provide scaling factors of the absolute flux levels applied to the spectra. We use the RMS of the zeropoints measured over the year as the typical uncertainty in the absolute flux calibration.

This uncertainty in the absolute flux calibration is recorded in the headers of all SOFI spectra with the following header keyword (as done for EFOSC2) :

```
FLUXERR = 22.0 /Fractional uncertainty of the flux [%]
```


3. SOFI imaging calibration frames and reduction

Bias, cross-talk and flat calibration : SOFI imaging is carried out as default when spectroscopy is done, providing images with a 4.9 arcmin field of view ($0.29 \text{ arcsec pix}^{-1}$). The cross talk effect is first corrected as for the spectra and all images are then flat fielded using dome flats, which are typically taken on an annual basis. Pairs of flats are taken with the dome screen illuminated and un-illuminated; the latter are then subtracted from the former to account for bias and thermal background. Multiple flats are combined, and then used to reduce the science data. An illumination correction is also applied, to account for the difference between the illumination pattern of the dome flats and the actual illumination of the night sky. The illumination correction is determined by imaging a bright star at each position in a 4×4 grid on the detector. The intensity of the star is then measured at each position, and a two-dimensional polynomial is fitted. This polynomial is normalised to unity, so that it can be applied to the imaging data as a multiplicative correction

Sky subtraction : For targets that are in relatively uncrowded fields, a dither pattern is employed where the telescope is moved to four offset positions on the sky, while keeping the target in the field of view (“on-source sky subtraction”). To determine the sky background, the four frames are then median combined without applying offsets, rejecting pixels from any individual image which are more than a certain threshold above the median. This initial sky image is subtracted from each individual frame in order to obtain a initial sky-subtracted images. These frames are used to identify the positions of all sources and create a mask frame for each science image. For each set of four images, the frames are then median combined again without applying offsets and using the masks created previously to reject all sources and produce the final sky image. The final sky background image is then subtracted from each of the input frames. The sky-subtracted images are then mosaiced together to create a single image using the *swarp* package (Bertin et al. 2002). For targets which are in a crowded field, or where there is extended diffuse emission (such as nearby galaxies), PESSTO observations alternate between observing the target, and observing an uncrowded off-source field around ~ 5 arcmin from the target (typically four frames on source, then four frames off source are observed, dithering in each case). The off-source frames are then used to compute a sky frame in the same way as for the “on-source sky subtraction”. The off-source sky frame is then subtracted from each of the on-source images of the target, which are then combined to create the final image. Since the field of view of SOFI is rather small (4.9 arcmin) the astrometry is not set for single images. Instead, *sExtractor* is run to detect sources in individual frames, and to check the nominal dither.

Astrometric calibration : The astrometric calibration was derived using the 2MASS reference catalogues, and a distortion model described by a second order polynomial. A typical scatter of 0.4-0.5 arcsec was been found for the science frames with around 15 stars usually recognised by the catalogue in the frame. This typically improves to an rms ~ 0.2 - 0.3 with $\sim >30$ stars.. The information on the RMS of RA and DEC

is provided in the standard CRDER1 and CRDER2 keywords and repeated, along with the number of stars used for the calibration, in the PESSTO-specific keyword ASTROMET.

Photometric calibration : The individual SOFI images, which themselves are the result of the average combination of NDIT images, are then mosaiced together in a median combine using *swarp*. An astrometric calibration is made, by cross correlating the sources detected by *sExtractor* with the 2MASS catalogue. The instrumental aperture magnitudes of the sources in the field as measured by *daophot* are then compared to their catalogued 2MASS magnitudes to determine the photometric zeropoint, which is recorded in the header of the image as *PHOTZP* without any further colour correction. The other relevant photometric keywords are as follows (see Smartt et al., 2015 for more details).

```
PSF_FWHM=          1.015714368/Spatial resolution (arcsec)
ELLIPTIC=          0.142 /Average ellipticity of point sources
PHOTZP =           25.4895217391 / MAG=-2.5*log(data)+PHOTZP
PHOTZPER=          0.09695742781/error in PHOTZP
FLUXCAL = 'ABSOLUTE' /Certifies the validity of PHOTZP
PHOTSYS = 'VEGA'    / Photometric system VEGA or AB
ABMAGSAT=          11.94145459901092/Saturation limit for point sources (AB mags)
ABMAGLIM=          18.96704572844871/ 5-sigma limiting AB magnitude for point sources
```

The zeropoint conforms to ESO SDP standards for archive images and can be employed simply as :

$$MAG = -2.5 \log(COUNTS_{ADU}) + PHOTZP$$

where $COUNTS_{ADU}$ is the measured signal in ADU. Users should be aware that these zeropoints are for guidance rather than for immediate and unchecked scientific use for photometry of transients. The zeropoints should always be checked with 2MASS sources, since the number and brightness of targets in automated selection varies considerably due to the limited field of view of SOFI.

SOFI artifacts and problem images : The SOFI images are characterized by a number of recurring features which are mostly related to the sky subtraction method employed above. For example, Fig 3 shows an example image and its weight to illustrate the “on-source sky subtraction”. Table 5 lists some specific example image issues from SOFI and the impact on their science use.

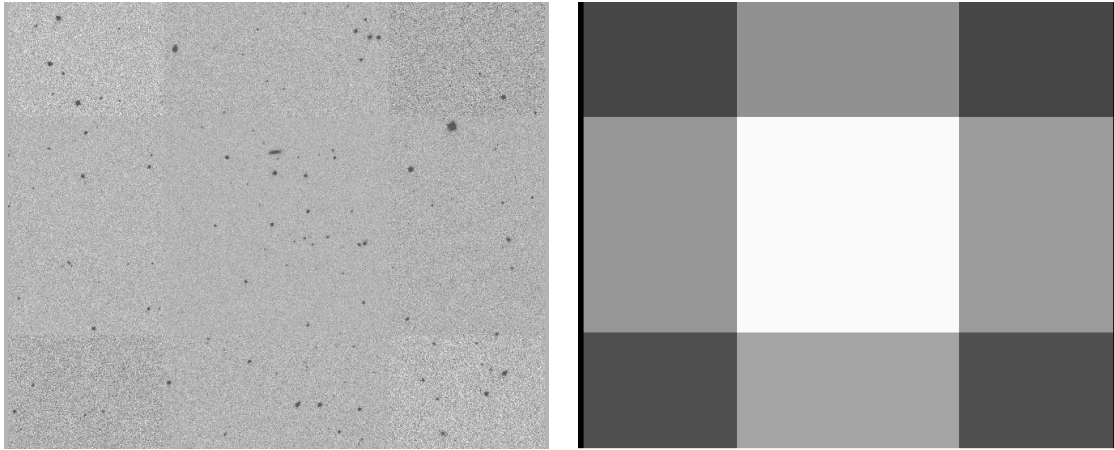


Fig 4 : the typical SOFI dither pattern for “on-source sky subtraction”. The left panel shows a typical image, with the sky noise levels varying due to the dither pattern illustrated. The right panel is the weight image.

Table 5 : Specific examples of SOFI imaging issues.

Images	Description of issues
SN2009ip_20131014_Ks_merge_57050_1.fits SN2013dn_20130816_H_merge_57049_1.fits SN2013ek_20130816_H_merge_57049_1.fits SN2013fs_20131014_Ks_merge_57050_1.fits	These exemplify cases where there are vertical noise patterns in the background, likely electronic in origin. However the middle region around the transient is typically less affected. These four are examples, there are others with similar background patterns.
OGLE-2013-SN-079_20131025_J_merge_57050_1.fits SN2013ek_20130828_J_merge_57049_1.fits SN2013fc_20131013_H_merge_57050_1.fits SN2013fc_20131209_Ks_merge_57050_1.fits	These exemplify cases where there are residuals from the bright host galaxy, when the offsets were used. This reflects the higher noise levels where the galaxy was shifted in the dither pattern. However the region around the transient should be unaffected. These four are examples, there are others with similar background patterns.
SN2012ca_20131102_H_merge_57050_1.fits SN2012ca_20131102_J_merge_57050_1.fits SN2013fc_20131003_H_merge_57050_2.fits SN2013fc_20131209_H_merge_57050_1.fits	Poor image, reason not known. Use with caution

SN2013ek_20130816_ks_merge_57049_1.fits
LSQ13ddu_20131209_H_merge_57050_1.fits

Core of a bright galaxy/star saturated. When the dithered offsets were used for sky subtraction, this prints through. However, the SN position should be unaffected. These two are examples, there are others with similar background patterns.

Previous Releases

Release DR1 contained flux-calibrated 1d EFOSC spectra of all targets taken during the first year (between April 2012 and April 2013), plus SOFI 1d spectra and imaging products for the brightest targets.

Release DR2 contained all the products of release number, 2 plus the 1d spectra and images of the targets taken during the second year (between August 2013 and April 2014), the first version of the PESSTO TRANSIENT catalogue, and the first version of the PESSTO MPHOT lightcurve catalogue.

List of Spectral Changes in DR2

1. Spectrum for object SN2103ek was re-uploaded to correct its object name to 'SN2013ek'.
2. Spectrum for object MASTER134201m023856 was re-uploaded to correct its object name to 'MASTERJ134201.21-023856.2'
3. Spectrum for object MASTEROTJ093953.18+165516.4 was re-uploaded to correct its object name to 'MASTERJ093953.18+165516.4'
4. Spectrum for object OGLE-2012-SN-027 was re-uploaded to correct its object name to 'OGLE-2012-SN-027'
5. Spectrum for object OGLE2013-SN-017 was re-uploaded to correct its object name to 'OGLE-2013-SN-017'
6. Spectrum for object PSNJ125333062742517 was re-uploaded to correct its object name to 'PSNJ12533306+2742517'
7. Spectrum for object PSNJ02554120-2725276 was re-uploaded to update its object name to 'SN2012fx'
8. Spectrum for object PSNJ04371913-6908254 was re-uploaded to update its object name to 'SN2012fu'
9. Spectrum for object PSNJ081753462328105 was re-uploaded to update its object name to 'SN2013gq'
10. Spectrum for object PSNJ09040080-7203248 was re-uploaded to update its object name to 'SN2013B'

11. Spectrum for object PSNJ19065165-6142163 was re-uploaded to update its object name to 'SN2012fv'
12. Spectrum for object PSNJ20032484-5557192 was re-uploaded to update its object name to 'SN2012fz'
13. Spectrum for object PSNJ21015899-4816259 was re-uploaded to update its object name to 'SN2012fw'
14. Spectrum for object PSNJ23054871+1419564 was re-uploaded to update its object name to 'SN2012ff'
15. Spectrum for object sn2012fs was re-uploaded to correct its object name to 'SN2012fs'
16. Spectrum for object sss121120-023241-391756 was re-uploaded to update its object name to 'SN2012hc'

Release DR3 contained all the products of DR2 plus the 1d spectra and images of the targets taken during the third and fourth years (between July 2014 and April 2016).

List of Spectral Changes in DR3

1. Spectrum for object SN2013gr taken on 21031221 was re-uploaded as the extracted source was that of the host galaxy and not the supernova.

Release DR3.1 contains all the products of DR3, plus the new version of the PESSTO catalogues.

List of Spectral Changes in DR3.1

1. The EFOSC spectrum for object PS15cyz was incorrectly associated with PS1-14og. The association has been corrected within the OBJECT keyword and spectral filename.
2. The EFOSC spectrum for object MASTERJ165420.77-615258 was incorrectly associated with PSNJ16541584-6153309. The association has been corrected within the OBJECT keyword and spectral filename.
3. The 2 SOFI spectra for object ASASSN-14ha were incorrectly associated with SN2010e1. Upon inspection, these spectra had very little signal from the transient object and have therefore been removed from the release.
4. The EFOSC spectrum for object SN2015R was incorrectly associated with SN2005G. The association has been corrected within the OBJECT keyword and spectral filename.
5. The EFOSC spectrum for object PS15afa was incorrectly associated with SN2008bt. The association has been corrected within the OBJECT keyword and spectral filename.
6. The EFOSC spectra for object PS15dqx was incorrectly associated with SN2005cd. The association has been corrected within the OBJECT keyword and spectral filename.
7. The EFOSC spectra for object SN2016P were incorrectly associated with SN2003b1. The association has been corrected within the OBJECT keyword and spectral filename.

8. The EFOSC spectrum for object ASASSN-15aj was incorrectly associated with SN2012bu. The association has been corrected within the OBJECT keyword and spectral filename.

List of Changes in DR4

1. Details of Gr#18 and Gr#20 added to Table 1 of the release description.
2. ASASSN-15fi, ASASSN-15pz, ASASSN-15rp, AT2016aqs, DES15S2nr, LSQ13ccw, LSQ14doz, PS15cel, PS15cem, PS15cko, SN2013F and SN2014da were removed from Table 4 of the release description as not enough data was taken of these objects to warrant follow-up status.
3. Host galaxy / transient associations are now preformed with the Sherlock crossmatch algorithm.
4. Removed the TRANSIENT_DISCOVERY_ID and HOST_SEARCH_STAGE from the PESSTO Transient Catalogue. The transient discovery ID is now absorbed into the TRANSIENT_ALTERNATIVE_IDS column.
5. A TRANSIENT_CLASSIFICATION_SPECTRUM column has been added to the PESSTO Transient Catalogue. The column records the ORIGFILE filename of the PESSTO spectrum used to determine a transient classification.

Data Format

1. EFOSC2 data file types and naming

One dimensional flux calibrated spectra are in binary table format and conform to the ESO Science Data Products Standard (Retzlaff et al. 2013). The binary table FITS file consists of one primary header (there is no data in the primary HDU so NAXIS=0), and a single extension containing a header unit and a BINTABLE with NAXIS=2. A unique FITS file is provided for each individual science spectrum. The actual spectral data is stored within the table as vector arrays in single cells. As a consequence, there is only one row in the BINTABLE, that is NAXIS2=1.

Information associated with the science spectrum is also provided within the same binary table FITS file resulting in a table containing one row with four data cells. The first cell contains the wavelength array in angstroms. The other three cells contain the science spectrum flux array (extracted with variance weighting), its error array (the standard deviation produced during the extraction procedure) and finally the sky background flux array. Each flux array is in units of $\text{erg cm}^{-2} \text{s}^{-1} \text{\AA}^{-1}$.

The science spectrum has a filename of the following form, object name, date of observation, grism, filter, slit width, MJD of data reduction date, a numeric counter (beginning at 1) to distinguish multiple exposures taken on the same night, and a suffix sb to denote a spectrum in binary table format.

SN2013ak_20130412_Gr11_Free_slit1.0_56448_1_sb.fits

In the few cases where the object name is longer than 20 characters, it is truncated within the filename to ensure the filename does not exceed the 68 character limit enforced by ESO. The full object name is always recorded in the OBJECT keyword.

They can be identified as having the data product category keyword set as

```
PRODCATG = SCIENCE.SPECTRUM /Data product category
```

The 2D spectrum images which can be used to re-extract the object as discussed above are released as associated ancillary data. They are associated with the science spectra through the following header keywords in the science spectra files. The file name is the same as for the 1D spectrum, but the suffix used is `i` to denote an image.

```
ASSOC1 = ANCILLARY.2DSPECTRUM /Category of associated file
ASSON1 = SN2013ak_20130412_Gr11_Free_slit1.0_56448_1_si.fits /Name of associated file
```

These 2D files are wavelength and flux calibrated hence a user can re-extract a region of the data and have a calibrated spectrum immediately. Users should note the value for `BUNIT` in these frames means that the flux should be divided by 10^{20} to provide the result in $\text{erg cm}^{-2} \text{s}^{-1} \text{\AA}^{-1}$.

2. SOFI data file types and naming

The data products for SOFI are similar to those described above for EFOSC2. The spectra are in binary table FITS format, with the same four data cells corresponding to the wavelength in angstroms, the weighted science spectrum and its error and the sky background flux array. Again, each flux array is in units of $\text{erg cm}^{-2} \text{s}^{-1} \text{\AA}^{-1}$. The SSDR1 FITS keywords described Smartt et al. (2015) are again applicable here. A typical file name is

```
SN2009ip_20130417_GB_merge_56478_1_sb.fits
```

Where the object name is followed by the date observed, the grism (GB for the blue grism, or GR for the red grism), the word “merge” to note that the individual exposures in the ABBA dither pattern have been co-added, the date the file was created, a numeric value to distinguish multiple exposures on the same night and a suffix `sb` to denote a spectrum in binary table format. As with EFOSC2, this science spectrum can be identified with the label:

```
PRODCATG = SCIENCE.SPECTRUM /Data product category
```

We also provide the 2D flux calibrated and wavelength calibrated file so that users can re-extract their object directly, as described with EFOSC2. The identification of the 2D images follow the same convention as for EFOSC2, with the suffix `si` to denote a spectral image.

```
ASSOC1 = ANCILLARY.2DSPECTRUM /Category of associated file
ASSON1 = SN2009ip_20130417_GB_merge_56478_1_si.fits /Name of associated file
```

In nearly all cases where PESSTO takes a SOFI spectrum, imaging in JHK_s is also taken. These images are flux and astrometrically calibrated and released as science frames. They are labeled as follows where K_s labels the filter and the `merge` denotes that the dithers have been median combined.

SN2013am_20130417_Ks_merge_56475_1.fits

We also release the image weight map as described in (Retzlaff et al. 2013). The definition in this document is the pixel-to-pixel variation of the statistical significance of the image array in terms of a number that is proportional to the inverse variance of the background, i.e. not including the Poisson noise of sources. This is labelled as

```
ASSOC1 = ANCILLARY.WEIGHTMAP /Category of associated file  
ASSON1 = SN2013am_20130417_Ks_merge_56475_1.weight.fits /Name of associated file
```

Catalogue Columns

This release contains the PESSTO Transient Catalogue which is a catalogue of all sources for which a meaningful spectral classification has been obtained up to April 2019. The columns are described in Table 7 below and we provide further explanatory information in this section.

1. Spectral classification

For spectral classification we chose the following standard classes (for TRANSIENT_CLASSIFICATION). Although other classification terms have been proposed (e.g. Iax, Ic-BL, SLSN-R, Ia+CSM, “Ca-rich”, .Ia etc) we have kept with the standard classification scheme with a Boolean flag to note if a transient appears peculiar or unusual for its standard class TRANSIENT_CLASSIFICATION_PECULIAR_FLAG). The ATel announcements carry textual information on objects. The classifications we apply are

SN Ia : type Ia supernova
SN Ib : type Ib supernova
SN Ic : type Ic supernova
SN Ibc : either type Ib or Ic, ambiguous which
SN Ibn : type Ib with narrow He lines
SN I : type I, but ambiguous whether it should be Ia, Ib or Ic
SN II : type II, as evidence by broad H-lines
SN IIP : type IIP as good match to well studied II-P SNe
SN IIb : type IIb supernova
SN IIIn : type II supernova, with narrow H-lines
SLSN II : superluminous supernova, with hydrogen lines visible
SLSN Ic : superluminous supernova, with no hydrogen or helium obvious visible in the optical
FRB : fast radio burst counterpart candidate
Galactic Nova : nova hosted within the Milky Way
Impostor : likely giant eruption or non terminal explosion of massive star
AGN : active galactic nucleus variability
CV : cataclysmic variable candidate
Variable star : a catch all for any type of variable or transient with zero redshift or negligible radial velocity
Galaxy : spectrum dominated by galaxy light
TDE : tidal disruption event

Unknown : unable to classify (e.g. the most common examples are blue featureless continuum objects)

2. Phase classification

We provide a general phase of classification of the transient spectrum, with respect to maximum light of the lightcurve for the type of object it is classified as. As there is some uncertainty in this procedure we adopt a two tiered approach to provide this information in a reliable form that respects the inherent uncertainty in phase classification. All transients are given one of the following values for TRANSIENT_CLASSIFICATION_PHASE :

Pre-max : transient is very likely caught before maximum light
 Max : transient is likely around maximum light
 Post-max : transient is very likely after maximum light
 Unknown : phase can not be discerned from the information in hand
 NULL : if the transient is not a supernova

If the transient phase can be further refined we provide the following ranges

Table 6. Ranges of phase classification provided

TRANSIENT_CLASSIFICATION_PHASE_DAYS_LOWER_LIMIT	TRANSIENT_CLASSIFICATION_PHASE_DAYS_UPPER_LIMIT
NULL	-10
-10	-8
-7	-4
-3	3
4	7
8	10
11	20
20	NULL

3. Host galaxy identification

A boosted decision tree algorithm (*Sherlock*) is used to generate the cross-matches between the transients and associated astrophysical sources. Sherlock mines a library of historical and on-going astronomical survey data (PS1 DR1, Gaia DR2, SDSS DR12, NED and more) and attempts to predict the nature of the object based on the resulting crossmatched associations found.

The bulk of transients are not in galaxies that have had previous spectroscopic redshifts measured. Hence we have also provided, where possible, a measurement of the photometric redshift (usually from SDSS DR12). This will be useful for future analysis to determine if photometric redshifts can be used in any way to determine the absolute magnitudes and luminosities of the transients.

4. List of column names and description

Table 7. Column description for the PESSTO transient object catalogue.

Field Name	Description
TRANSIENT_ID	The master transient ID as found in the spectral and imaging data and the multi-epoch photometry catalogue (PESSTO_MPHOT)
TRANSIENT_IAU_ID	The official IAU designation given to the transient if it exists.
TRANSIENT_ALTERNATIVE_IDS	All designations assigned to the transient by surveys other than the discovery survey.
TRANSIENT_RAJ2000	RA of the transient in decimal degrees. This generally comes from the original survey discovery
TRANSIENT_DECJ2000	DEC of the transient in decimal degrees. This generally comes from the original survey discovery
TRANSIENT_CLASSIFICATION	The classification of the transient. These are generally from the PESSTO ATel announcements, with some updates based on PESSTO data coverage. For this catalogue PESSTO has adopted standard classification labels, discussed later in this section of the release description.
TRANSIENT_CLASSIFICATION_PECULIAR_FLAG	Boolean flag, set to "1" if transient classified as peculiar (for its particular spectral classification)
TRANSIENT_CLASSIFICATION_SOURCE	The source of the classification. Most sources in this catalogue were classified by PESSTO but some objects were observed after third party classifications. In those cases, the originating ATels or CBETs are referenced.
TRANSIENT_CLASSIFICATION_ATEL	The ATel reference reporting the classification
TRANSIENT_CLASSIFICATION_MJD	MJD at the point of classification

TRANSIENT_CLASSIFICATION_REDSHIFT	The redshift of the transient measured from the classification spectra
TRANSIENT_CLASSIFICATION_PHASE	The phase of the transient at classification with respect to maximum light in days (see below for a discussion on this)
TRANSIENT_CLASSIFICATION_PHASE_DAYS_LOWER_LIMIT	Estimated Lower limit of the phase of the transient (days)
TRANSIENT_CLASSIFICATION_PHASE_DAYS_UPPER_LIMIT	Estimated Upper limit of the phase of the transient (days)
TRANSIENT_CLASSIFICATION_SPECTRUM	The ORIGFILE filename of the PESSTO spectrum used to determine the transient classification.
TRANSIENT_DISCOVERY_MJD	MJD at the point of discovery, reported from the originating discovery survey
TRANSIENT_DISCOVERY_MAG	Magnitude of the transient at the point of discovery, reported from the originating discovery survey
TRANSIENT_DISCOVERY_MAG_FILTER	Filter that TRANSIENT_DISCOVERY_MAG was reported in, from the originating discovery survey
FOLLOWUP_TARGET	Boolean flag, set to "1" if transient became a PESSTO target for time series follow-up
HOST_ID	The name of an associated host galaxy, if identified
HOST_RAJ2000	RA of host galaxy in decimal degrees
HOST_DECJ2000	DEC of host galaxy in decimal degrees
HOST_OFFSET_N	The N-S transient-host separation (in decimal degrees). Positive means the transient is North of the host.
HOST_OFFSET_E	The E-W transient-host separation (in decimal degrees). Positive means the transient is East of the host
HOST_REDSHIFT_SPEC_SOURCE	Catalogue source of the host galaxy's spectroscopic redshift
HOST_REDSHIFT_SPEC	Host galaxy spectroscopic redshift
HOST_REDSHIFT_PHOT_SOURCE	Catalogue source of the host galaxy's photometric redshift

HOST_REDSHIFT_PHOT	Host galaxy photometric redshift
HOST_REDSHIFT_PHOT_ERR	Host galaxy photometric redshift error

Acknowledgements

If using these data, please cite this paper

Smartt S.J. et al. 2015, A&A, 579, 40: PESSTO: survey description and products from the first data release of the Public ESO Spectroscopic Survey of Transient Objects

And please also add the following acknowledging statement in your articles

Based on data products from observations made with ESO Telescopes at the La Silla Paranal Observatory under programmes 188.D-3003 and 191.D-0935: PESSTO (the Public ESO Spectroscopic Survey for Transient Objects).

References

- Barabbarino C. et al., 2015, MNRAS, 448, 2312
 Bennetti S., et al., 2014, MNRAS, 441, 289
 Bertin, E., Mellier, Y., Radovich, M., et al. 2002, in Astronomical Society of the Pacific Conference Series, Vol. 281, Astronomical Data Analysis Software and Systems XI, ed. D. A. Bohlender, D. Durand, & T. H. Handley, 228
 Childress M., et al. 2013, ApJ, 770, 29
 Childress M., et al. 2015, MNRAS, 454, 3816
 Fraser M., et al. 2013, MNRAS, 433, 1312
 Fraser M., et al. 2015, MNRAS, 453, 3886
 Gall E. E. E., et al. 2015, A&A, 582, A3
 Hosseinzadeh G., et al. 2016, ApJ, in press, arXiv:1608.01998
 Inserra, C., et al. 2013, MNRAS, 770, 128
 Inserra, C., et al. 2013, MNRAS, 459, 2721
 Inserra C., et al. 2016, ApJ, submitted, arXiv:1604.01226
 Jerkstrand A., et al., 2015, MNRAS, 448, 2482
 Jerkstrand A., et al., 2016, ApJ, arXiv:1608.02994
 Jester et al. 2005, AJ, 130, 873
 Kangas T., et al. 2016, MNRAS, 456, 323
 Magee M., et al., 2016, A&A, 589, A89
 Maguire K., et al. 2013, MNRAS, 436, 222
 Maund J.R. et al. 2013, MNRAS, 431, L102
 Nicholl et al. 2014, MNRAS, 444, 2096
 Nicholl M., et al. 2015, ApJ, 807, L18
 Nicholl M., et al. 2016a, ApJ, 826, 39
 Nicholl M., et al. 2016b, ApJ, in press, arXiv:1608.02995
 Pastorello A., et al. 2015a, MNRAS, 449, 1941
 Pastorello A., et al. 2015b, MNRAS, 449, 1954
 Polshaw J., et al. 2016, A&A, 58, A177
 Retzlaff et al. 2013, GEN-SPE-ESO-33000-5335, Issue 5
 Scalzo R., et al. 2014, MNRAS, 445, 30
 Smartt S.J. et al. 2015, A&A, 579, 40

van Dokkum, P. G. 2001, PASP, 113, 1420
Yaun F. et al. 2016, MNRAS, 461, 2003
Wyrzykowski L., et al., MNRAS, submitted